Journal of Materials Chemistry

Cite this: *J. Mater. Chem.*, 2012, **22**, 1928

www.rsc.org/materials

PAPER

Interface molecular engineering of single-walled carbon nanotube/epoxy composites†

Yehai Yan,* Jian Cui, Shuai Zhao, Jinfang Zhang, Jiwen Liu and Junmei Cheng

Received 1st September 2011, Accepted 28th October 2011
DOI: 10.1039/c1jm14310g

Dispersion of large single-walled carbon nanotube (SWCNT) bundles into individual nanotubes or small bundles and thus strengthening of the nanotube/matrix interfacial interaction are prerequisites for taking full advantage of the remarkable multifunctional properties of SWCNTs in various carbon nanotube-based composites. Noncovalent functionalization of SWCNTs is an attractive option to simultaneously achieve these conditions. Toward this end, three reactive amino-containing pyrene derivatives (AmPys) with various spacer chain lengths were synthesized. One with the longest spacer length (12 methylene units, AmPy-12) shows the highest functionalization efficiency for SWCNTs in terms of dispersibility. Systematic characterization on a SWCNT/AmPy-12 hybrid suggests that *ca.* 10 wt% of AmPy-12 is strongly adsorbed on SWCNTs through π–π interactions, making them steadily dispersed into individual ones and/or small bundles without noticeable change in their electronic structure. AmPy-12-functionalized SWCNTs were then used for the preparation of epoxy composites. Since the SWCNT/epoxy interface was well engineered at a molecular level by application of AmPy-12, which interacts noncovalently with SWCNT but bonds chemically to the epoxy matrix, the composite with only 0.3 wt% SWCNTs displays an increase of 54% and 27% in tensile strength and Young's modulus, respectively, over neat resin. A low electrical percolation threshold of 0.1 wt% SWCNTs and improved thermal properties were also observed.

1. Introduction

A high aspect ratio (1000 or more) together with low density and high strength render carbon nanotubes (CNTs) ideal reinforcing fillers in polymer composites. More intriguing is that the excellent mechanical, thermal and electrical properties of CNTs afford great opportunities for multifunctional materials.[1–4] However, an amount of work remains to be done before actualizing the full potential of nanotube composites. The researchers still face challenges, such as homogeneously dispersing CNTs (perfectly down to an individual nanotube level) in the polymer matrix and strengthening the CNT/matrix interfacial interaction. For a high-quality composite, the former is a prerequisite, but not yet substantial. This is because the atomically smooth surface and chemical inertness of pristine CNTs induce weak interfacial adhesion with the matrix, thus making load transfer from the matrix to the nanotubes very poor. Functionalization of CNTs has proven to be an effective means to improve the dispersibility of CNTs and, more importantly, enable engineering of the nanotube/polymer interface at a molecular level for strong interfacial interactions.[5–9]

Of the available functionalization methods, covalent attachment of functional groups on the nanotube surface is the most commonly used strategy. Mechanical enhancements of the resultant composites were generally achieved, however, this was at the cost of the electrical and thermal properties of CNTs. On the contrary, noncovalent methods based mainly on van de Waals interactions are well-known to preserve nearly all of the intrinsic features of CNTs. Although such methods are usually not as powerful as covalent ones in terms of mechanical enhancement of CNT/polymer composites, multifunctional materials, *e.g.* electrically conductive polymer composites with modestly enhanced mechanical performance, are available. In a typical work, CNTs were noncovalently functionalized by poly (vinylbenzyl oxyethyl naphthalene)-*g*-poly(methyl methacrylate) and used in the matrix of poly(styrene-*co*-acrylonitrile).[10] Since the crucial issues of nanotube dispersion and interfacial interaction have been satisfactorily resolved without damaging the nanotube's electronic structure, the resultant composites displayed significantly improved mechanical and electrical properties as compared with neat polymer and composites filled with pristine CNTs. The multifunctional composites have also been achieved in the matrices of polycarbonate,[11] Parmax[8] and

Key Laboratory of Rubber-plastics, Ministry of Education/Shandong Provincial Key Laboratory of Rubber-plastics, College of Polymer Science and Engineering, Qingdao University of Science and Technology, Qingdao, 266042, China. E-mail: yhyan@qust.edu.cn; Fax: +86-532-8402 3977; Tel: +86-532-8402 2416

† Electronic supplementary information (ESI) available: See DOI: 10.1039/c1jm14310g

polyimide,[12] where CNTs noncovalently functionalized by poly (3-hexylthiophene)-*g*-polycaprolactones, poly(*p*-phenylene ethynylene) and polyimide were used as fillers, respectively. To date, noncovalent strategies have made much progress in thermoplastic matrices, but only a few studies addressed thermosetting ones.[13]

Epoxy resin is a well-established thermoset with a wide range of applications from electronics to aerospace. Despite their favorable mechanical performance and good chemical and corrosion resistance, technological advances have put forward multifunctional requirements on the epoxy-based materials and there are practical demands on electrical conductivity and improved mechanical properties. Filling epoxy resin with noncovalently functionalized CNTs seems to be an attractive option for such an objective. Surfactants,[14,15] protein,[16] gum Arabic[17] and polyimide-*g*-bisphenol A diglyceryl acrylate[13] have been explored for the noncovalent functionalization of CNTs, which were then used for the preparation of epoxy composites. Unfortunately, the mechanical or electrical performance of these materials have only been measured individually, and both have not been assessed together in the same work. Recently, Grunlan and co-workers[18] have prepared epoxy composites using polyethyleneimine as a noncovalent dispersant of CNTs. Their study suggested that both the electrical conductivity and storage modulus were similar to those of the composites based on pristine CNTs and there was hardly any performance improvement. The development of multifunctional CNT/epoxy composites is still an open problem.

This paper presents the design, synthesis and application of amino-containing pyrene derivative (AmPy) as a reactive noncovalent functionalization agent for single-walled carbon nanotubes (SWCNTs). As depicted in Fig. 1, the pyrene units make AmPy strongly interact with the nanotubes through a noncovalent interaction, whereas the alkylamine species facilitate dispersion of nanotubes and readily react with epoxy. Once the functionalized SWCNTs are added into epoxy system (including bisphenol-A-diglycidyl ether as resin and triethylenetetramine as hardener), the amino groups in AmPy enable SWCNTs to be seamlessly connected to the epoxy network and become an integral part of the resultant composite. In order to implement this novel design of a SWCNT/epoxy interface at a molecular level through a noncovalent strategy, three AmPys with various spacer chain lengths were first synthesized and characterized. The functionalization effect of AmPy on SWCNTs was then systematically assessed by diverse characterization techniques. Finally, the SWCNT/epoxy composites were prepared by a solution-based process and their mechanical, electrical and thermal properties were measured as a function of nanotube content. To the best of our knowledge, there are few reports thus far on applying a pyrene derivative to the nanotube/epoxy composite, although various pyrene derivatives have been previously used in thermoplastic matrix composite systems.[19–23] Compared with pristine SWCNTs, AmPy-functionalized SWCNTs have shown higher efficacy for physical performance enhancements. Multifunctional, but lightweight epoxy composites are hence at hand.

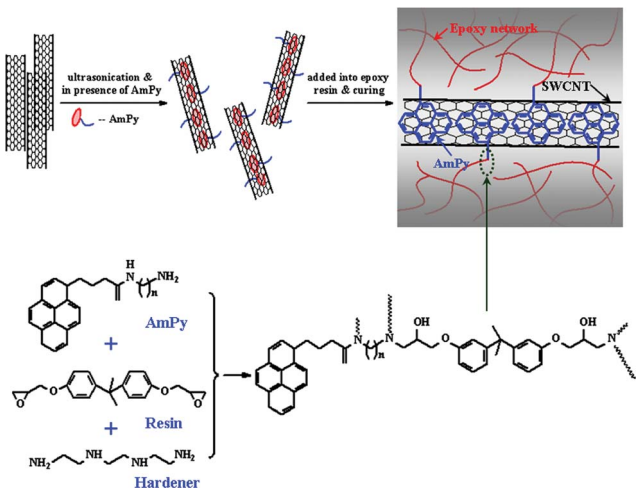

Fig. 1 Interface molecular engineering of the SWCNT/epoxy composite by application of AmPy.

2. Experimental

2.1 Materials

SWCNTs (purity >90%, diameter 1–2 nm, length 1–3 μm) produced by a conventional chemical vapor deposition (CVD) process were purchased from Timesnano Inc., China. Epofix from Struers was used as the epoxy matrix. It was supplied in two parts: Epofix hardener (triethylenetetramine) and Epofix resin containing 60–90% of bisphenol-A-diglycidylether ($\overline{M_n} \leq 700$) and 10–40% of alkyl (C12–C14) glycidyl ether. 1-Pyrenebutyric acid, *N*-hydroxysuccinimide and 1-ethyl-3-(3-dimethylaminopropyl) carbodiimide hydrochloride (EDC·HCl) were bought from Aldrich. Ethylenediamine, 1,6-diaminohexane, 1,12-diaminododecane and triethylamine were supplied by Aladdin Reagent, China.

2.2 Synthesis of pyrenebutyric acid *N*-hydroxysuccinimide ester (PyHSE)

EDC·HCl (3.0126 g, 15.7 mmol) was dissolved in anhydrous dichloromethane (100 ml) and then added dropwise into a solution of 1-pyrenebutyric acid (4.1670 g, 14.5 mmol) and *N*-hydroxysuccinimide (1.9760 g, 17.2 mmol) in the same solvent (150 ml) at 0 °C. After being stirred for 30 min, the reaction mixture was warmed up to room temperature and the reaction was allowed to remain at this temperature for 24 h. The final reaction solution was washed using ultrapure water (3 × 125 ml). After drying over $MgSO_4$ for 1 h, the organic solution was filtered and dichloromethane was evaporated. The crude product was dissolved in 5 ml tetrahydrofuran (THF) and recrystallized by the addition of 20 ml hexane. After leaving in a −20 °C freezer for 12 h, the solid was collected by filtration. The recrystallization process was repeated another two times. Finally, the collected solid was dried in a 50 °C vacuum oven for 6 h (yellow solid, 92% yield). Proton nuclear magnetic resonance (^{1}H-NMR) spectroscopy (δ, ppm, Fig. 2): 7.82–8.24 (*a*), 3.40–3.44 (*b*), 2.80 (*c*), 2.66–2.69 (*d*), 2.23–2.27 (*e*); Fourier transform infrared (FTIR) spectroscopy (υ, cm^{-1}): 1739 (ester carbonyl), 1780 (imide carbonyl).

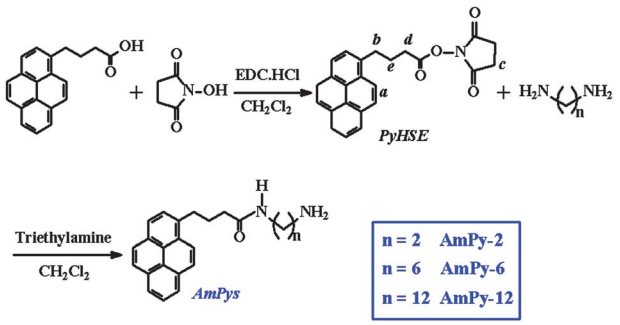

Fig. 2 The synthesis of AmPy.

2.3 Synthesis of AmPys

In a typical experiment, PyHSE (1.5012 g, 3.9 mmol) was dissolved in chloroform (85 ml) and then slowly added into the solution of ethylenediamine (2.2 ml, 32.9 mmol) and triethylamine (4.5 ml, 32.3 mmol) in the same solvent (15 ml) over 2.5 h at 0 °C. After being stirred for a further 30 min, the reaction mixture was warmed up to room temperature and the reaction was allowed to continue for 24 h. The reaction solution was filtered and the filtrate was washed using ultrapure water (3 × 50 ml). After drying over $MgSO_4$, the organic solution was filtered and chloroform was evaporated. The crude product was dissolved in 3 ml THF and recrystallized at −20 °C overnight. After filtration, the solid was thoroughly washed using hexane and dried in a 50 °C vacuum oven for 6 h. All three AmPys are pale yellow solids with yields of 85%, 65% and 68% for AmPy-2, AmPy-6 and AmPy-12, respectively.

2.4 Dispersion of pristine SWCNTs

SWCNTs (0.2 mg ml^{-1}) were dispersed in THF by mixing with a calculated content of AmPy followed by ultrasonication (Yuhua KQ250B, 40 kHz) for 2 h with the water bath temperature maintained at around 20 °C. The dispersion was allowed to settle for 24 h and 3/4 supernatant was carefully drawn out and passed through densely packed glass wool to remove the big aggregates. The uniform and dark dispersion thus collected was used in the optimization study of AmPys, *i.e.*, for the measurements of nanotube dispersibility and dispersion stability.

For other work, SWCNTs (74 mg L^{-1}) were dispersed in THF by mixing with AmPy-12 (0.08 mg ml^{-1}) followed by ultrasonication in a water bath for 2 h. The thus-obtained dispersion can be directly used for the composite preparation. For assessing the effect of AmPy-12 on the dispersion of SWCNTs (*i.e.*, for the characterization of atomic force microscopy (AFM), ultraviolet-visible-near infrared (UV-Vis-NIR) and fluorescence spectroscopy), however, the dispersion should undergo the following process to remove the free AmPy-12. After filtration over a 1.0 μm PTFE membrane (Millipore), the filter cake was redispersed in fresh THF by ultrasonication for 5 min. The dispersion was then filtrated again. The process was repeated several times until no AmPy-12 could be detected by UV spectroscopy in the filtrate. The collected black solid was dried in a 50 °C vacuum oven for 6 h and named as SWCNT/AmPy-12 hybrid.

2.5 Preparation of composites

For the preparation of the SWCNT/EP–AmPy-12 composites, Epofix resin was mixed with the SWCNT dispersion in a ratio to yield the expected content of SWCNTs. The mixture was strongly stirred for 30 min, followed by ultrasonication in a water bath for 1 h. After removal of THF by rotary evaporation, the hardener was added at a weight ratio of resin/hardener = 25 : 3. The mixture was stirred for 3 min, cast into silicon rubber mold (60 mm × 60 mm × 1 mm) and degassed in a vacuum oven. The final mixture was cured at 50 °C for 12 h and 80 °C for 2 h. As indicated by the FTIR spectra of the cured samples, in which the bands for epoxy groups (912 cm^{-1}) completely disappeared (Fig. S1†), the curing cycle adopted here ensures that the epoxy system and its composites are fully cured. The SWCNT/EP composites were also prepared using the same process.

2.6 Characterization

^{1}H-NMR (500 MHz, $CDCl_3$/DMSO-d_6) spectra were recorded on a Bruker AV500 spectrometer. FTIR spectra were obtained using a Bruker VERTEX 70 spectrometer in the Attenuated Total Reflectance (ATR) mode. AFM measurements were performed with a Multimode scanning probe microscope equipped with a Nanoscope IIIa controller. UV-Vis and UV-Vis-NIR spectra were collected using a TU-1800PC spectrophotometer and a Varian Cary 500 spectrophotometer, respectively. Fluorescence spectra and decay curves were recorded on a HITACHI F-4600 spectrophotometer and an Edinburgh Instrument FLS 920 spectrophotometer, respectively, with an excitation wavelength of 344 nm. Differential scanning calorimetry (DSC) was conducted on a TA Instruments DSC Q20 in a nitrogen atmosphere with a heating rate of 10 °C min^{-1}. The fracture surface of composites was observed using a JEOL JSM-7500F scanning electron microscope (SEM). For the tensile test, the composites were cut into rectangular specimens measuring 60 mm × 10 mm × 1 mm. The tensile properties were evaluated using a Zwick/Roell Z030 universal testing machine at a crosshead speed of 5 mm min^{-1}. All electrical conductivity measurements were performed at room temperature and 50% relative humidity. The volume conductivity lower than 10^{-5} S cm^{-1} was measured using a PC68 high resistance meter, while that higher than 10^{-5} S cm^{-1} was measured by a standard four-probe method using a MODEL SZT-2000 instrument.

3. Results and discussion

AmPys were synthesized through an amidation reaction between 1-pyrenebutyric acid and diamine (Fig. 2). The FTIR and ^{1}H-NMR spectra for a typical AmPy, *i.e.* AmPy-2, are given in Fig. 3. The peaks centered at 3291, 1655 and 1544 cm^{-1} in the FTIR spectrum correspond to –NH– stretching, C═O stretching and C–N–H bending, respectively, evidencing the formation of a secondary amide group. The presence of the characteristic band of $–NH_2$ (3415 cm^{-1}) reveals that the desired asymmetric amidation was realized by adding the intermediate of PyHSE into equimolar diamine as slowly as possible. Moreover, the multi-peaks at 7.95–8.41 ppm in the ^{1}H-NMR spectrum make clear that the pyrene unit is truly included in the molecular structure of AmPy-2. Similar FTIR and ^{1}H-NMR spectral features are also

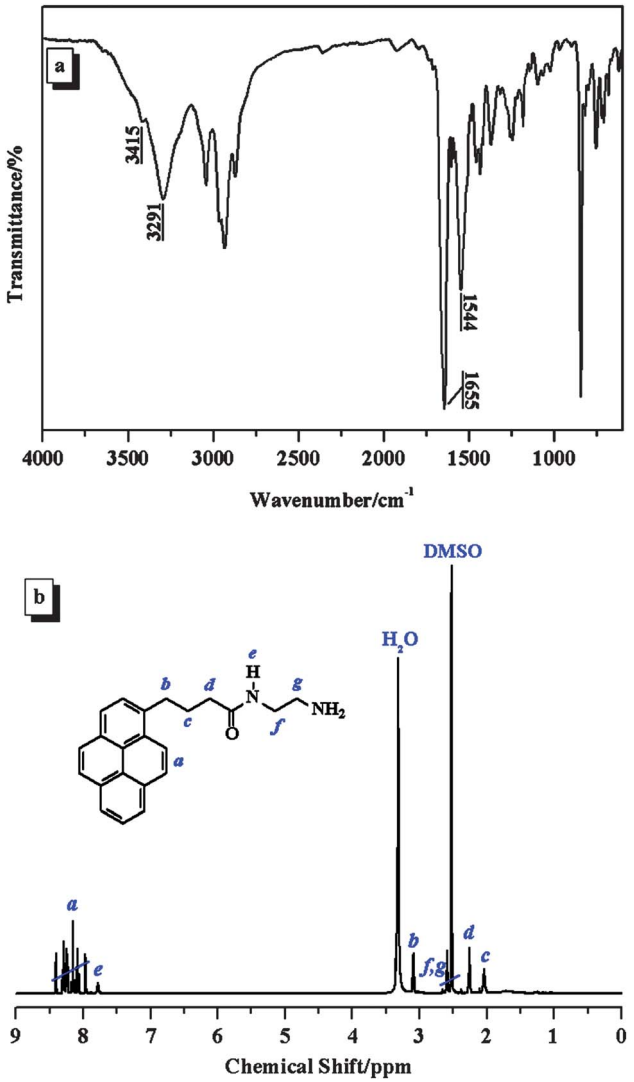

Fig. 3 (a) FTIR and (b) ^{1}H-NMR spectra of AmPy-2.

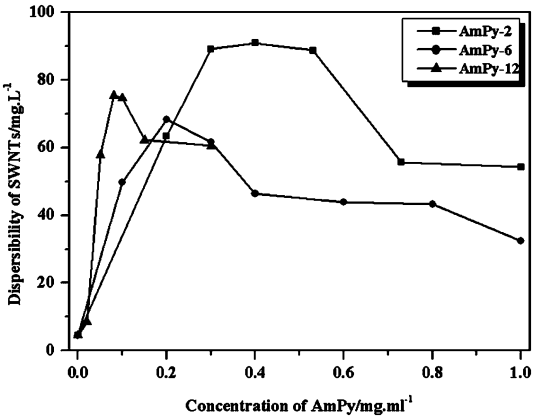

Fig. 4 Dispersibility of SWCNTs as a function of the mass concentration of AmPy.

observed for AmPy-6 and AmPy-12, thus suggesting that the amino-containing pyrene derivatives were successfully synthesized. It should be noted that the process for the synthesis of AmPys presented here is relatively complex and could be a drawback for a large scale production. As a promising alternative, in future work, 1-pyrenecarbaldehyde may be used to replace 1-pyrenebutyric acid, so that the AmPy can be simply synthesized in one step (Fig. S2†).

The AmPy compounds were then used for noncovalent functionalization of SWCNTs. A well developed UV-Vis spectroscopy-based method with a previously determined specific extinction coefficient of $\varepsilon_{500} = 0.021$ is adopted here for measuring the dispersibility of SWCNTs in THF.[24,25] As shown in Fig. 4, the dispersibility shows a strong dependence on the concentration of AmPy. Only 4.5 mg L^{-1} of uniform dispersion can be formed in pure THF. In the presence of AmPy, however, this value increases up to a maximum of 91.0 mg L^{-1} for AmPy-2 at a concentration of 0.4 mg ml^{-1}, 68.4 mg L^{-1} for AmPy-6 at 0.2 mg ml^{-1}, or 75.4 mg L^{-1} for AmPy-12 at 0.08 mg ml^{-1}. Interestingly, further increasing the AmPy concentration beyond its optimum causes a decrease of the dispersibility. A similar tendency was also observed using sodium dodecyl sulfate (SDS) as a dispersant for SWCNTs in water.[26] Van der Waals- and depletion-induced aggregation mechanisms have been suggested there to explain the experimental fact that the SWCNT dispersibilities are relatively lower at low or high SDS concentrations. In the present case, the AmPy molecules are adsorbed on the nanotube surface and their adsorption and desorption behaviors in dispersions are parallel and competitive. At low concentrations, adsorption predominates over desorption so that the amount of AmPy adsorbed on the nanotube surface quickly increases with increasing AmPy concentration. The adsorbed AmPy molecules induce steric repulsion against van der Waals interactions among nanotubes, thus improving the nanotube dispersibility. Beyond a critical concentration (0.4 mg ml^{-1} for AmPy-2, 0.2 mg ml^{-1} for AmPy-6 and 0.08 mg ml^{-1} for AmPy-12), the excessive AmPy molecules may possibly self-organize into some supramolecular structures due to strong π-stacking interaction between pyrene units (Fig. S3†).[27] These structures prefer to approach each other to maximize the entropy of the whole system, rather than fit into two adjacent individual nanotubes or bundles. As a result, the approach generates a depletion attraction[28] that is presumably responsible for the decreased dispersibility at the high AmPy concentration.

For the AmPy-functionalized SWCNTs, the highest dispersibility takes place in the presence of AmPy-2, but the optimal AmPy-2 mass concentration is also the highest among the three AmPys (Fig. 4 and Table 1). Once the mass concentration of AmPy is converted to the molar concentration of pyrene unit and the dispersibility is redefined as nanotube content per molar pyrene unit, the renewed dispersibility was found in an ascending order of AmPy-2, AmPy-6 and AmPy-12. Namely, AmPy-12 holds the highest functionalization efficiency for SWCNTs in terms of dispersibility. Furthermore, the dispersion-containing AmPy-12 displays the most excellent stability. After being centrifuged at 3000 rpm for 30 min, the nanotube content in the upper clear liquid phase was measured to be 63.2 mg L^{-1} using the UV-Vis spectroscopy-based method mentioned above. For the dispersions based on AmPy-6 and AmPy-2, however, the corresponding values are 37.2 and 15.0 mg L^{-1}, respectively. The longest methylene chain length of AmPy-12 provides the biggest

Table 1 The dispersibility of SWCNTs at the optimal concentration of AmPy

AmPy	Optimal mass concentration of AmPy/mg ml^{-1}	Dispersibility of SWCNTs/mg L^{-1}	Molar concentration of pyrene unit/mmol L^{-1}	SWCNT content per molar pyrene unit/g mol^{-1}
AmPy-2	0.4	91.0	1.21	75.2
AmPy-6	0.2	68.4	0.52	132.3
AmPy-12	0.08	75.4	0.17	443.4

spatial volume in dispersion to impart strongly repulsive forces onto nanotubes *via* steric hindrance against re-agglomeration. In consideration of both functionalization efficiency and dispersion stability, the dispersion containing 75.4 mg L^{-1} of SWCNTs and 0.08 mg ml^{-1} of AmPy-12 is preferred in the subsequent experimental work.

To further assess the effect of AmPy on the dispersion of SWCNTs, the free AmPy-12 molecules that are not adsorbed on the nanotube surface were eliminated by a repeated process of ultrafiltration and filter cake re-dispersion. The collected solid is hereafter named a SWCNT/AmPy-12 hybrid. For AFM observation, the hybrid was redispersed in fresh THF and several drops of the dilute dispersion were spin-coated (4000 rpm/2 min) onto a cleaned silicon wafer. As revealed by Fig. 5, the nanotubes are reliably involved in the dispersion and are well-dispersed. The near-round particles in the AFM image are impurities, such as amorphous carbon material and metal catalysts used for the SWCNT synthesis. Statistics on the height of 30 various tubular structures in Fig. 5 indicate that the hybrid is a mixture of individual nanotubes (1.6 ± 0.6 nm of diameter) and their 3–5 nm bundles decorated with AmPy-12. The AmPy-12 content in the hybrid was quantitatively determined by the UV-Vis spectroscopy-based method. For this purpose, the molar extinction coefficient of AmPy-12 at 344 nm in THF was first established to be 4.96 × 10^4 M^{-1} cm^{-1} according to Lambert-Beer law. By comparing the concentrations of AmPy-12 in the feed and the filtrate liquid, the AmPy-12 content in hybrid is finally calculated to be 9.6 wt%.

It is unquestionable that AmPy-12 is adsorbed on the nanotube surface in a noncovalent fashion. However, this naturally raises the question of what is the exact nature of the nanotube/AmPy-12 interaction? As a powerful tool, fluorescence spectroscopy was used to address this issue. After being excited at a maximum adsorption wavelength of 344 nm, the AmPy-12 solution in THF (1 μg ml^{-1}) exhibits the strong characteristic fluorescence of pyrene with distinct peaks at 376, 387, 397 and 417 nm (Fig. 6a). Similar spectral features are also observed in the dispersion of the SWCNT/AmPy-12 hybrid (1 μg ml^{-1} of AmPy-12, Fig. 6a inset). For molecular pyrene, the intensity ratio of the peak centered at 376 nm to that at 387 nm, commonly known as I_1/I_3 ratio, has been suggested to provide information on the polarity of the medium surrounding the pyrene.[29,30] It is thus expected that the I_1/I_3 ratio of the SWCNT/AmPy-12 hybrid should be different from that of AmPy-12, reflecting the change

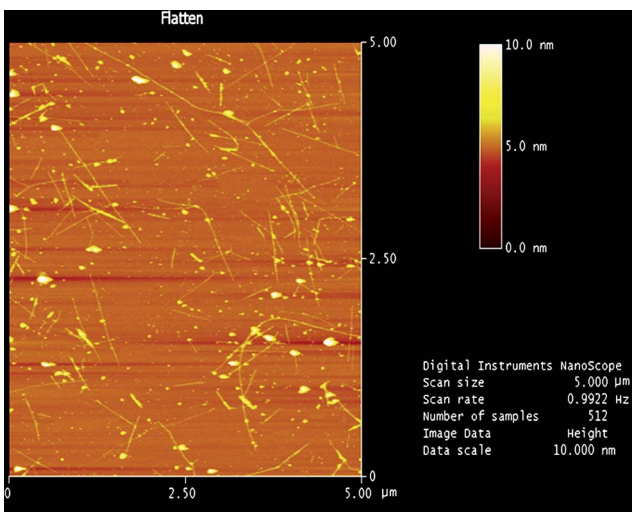

Fig. 5 A typical AFM image of the SWCNT/AmPy-12 hybrid.

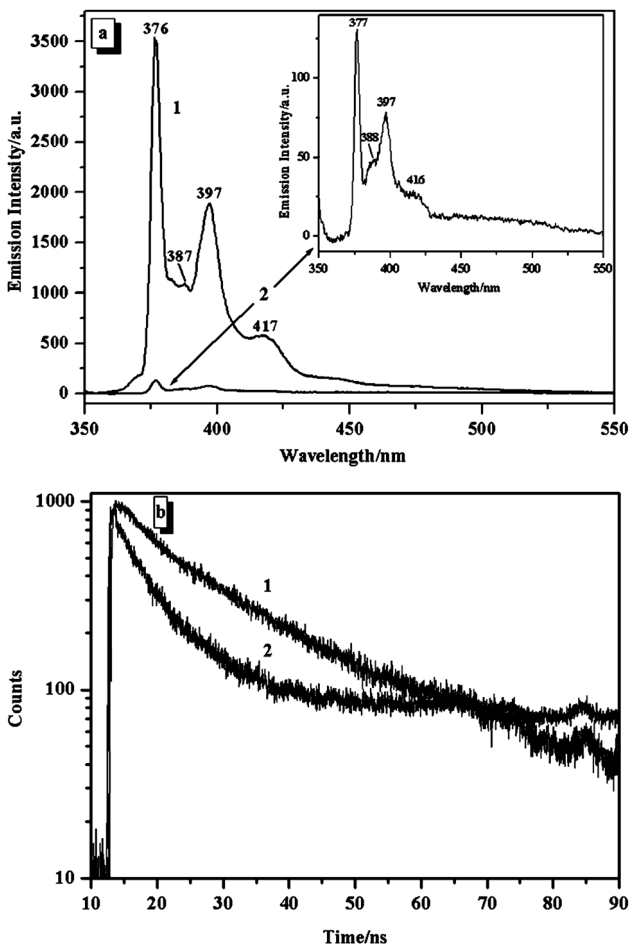

Fig. 6 (a) Fluorescence spectra (excited at 344 nm) and (b) decay curves of emission recorded at 397 nm of (1) AmPy-12 solution and (2) SWCNT/AmPy-12 dispersion in THF with the same AmPy-12 concentration of 1 μg ml^{-1}.

of the local environment of the pyrene moiety. However, AmPy-12 and the SWCNT/AmPy-12 hybrid show the almost same I_1/I_3 values of 1.29 and 1.31, respectively, which are quite close to I_1/I_3 = 1.35 for molecular pyrene[29] in the same solvent of THF. Although the mechanism for producing such a puzzling result is not yet clear, it does suggest that the I_1/I_3 ratio is not sensitive to the noncovalent interaction of SWCNTs with pyrene moieties. It is fortunate that the fluorescence intensity is strongly dependent on this interaction. Determined from the emission peak area, 95% of the fluorescence emission is quenched in the SWCNT/AmPy-12 hybrid with respect to that of AmPy-12. Actually, such a quenching effect has also appeared in other CNT/pyrene derivative systems and is widely accepted as evidence of the π–π interaction between nanotubes and pyrene derivatives.[22,23,31–34]

In order to provide further evidence, emission lifetime measurements were carried out on the same samples. Fig. 6b gives the temporal profiles of emission recorded at 397 nm upon excitation at 344 nm. Compared with AmPy-12, the hybrid shows a much faster emission decay and its fluorescence lifetime has shortened to 7.8 ns from 24.6 ns for AmPy-12, again suggesting that the pyrene emission is quenched by SWCNTs. The kinetic behavior, hence, provides a firm indication that there exists a strong molecular level interaction, *i.e.* π–π interactions, between SWCNT and AmPy-12.

The remarkable electrical conductivity of SWCNTs stemming from their unique electronic structure is highly desired for multifunctional composites. UV-Vis-NIR measurements were carried out to examine the electronic structure of the SWCNTs before and after the adsorption of AmPy-12 (Fig. 7). The absorption features within the recorded wavelength range of 400–1600 nm are usually interpreted as the interband electronic transitions of SWCNTs:[35] first transitions for metals (M11, 400–550 nm) and first and second transitions for semiconductors (S11, 850–1600 nm; S22, 550–850 nm). No evident spectral differences were noticed between the SWCNTs and hybrid. The strong π–π interactions between the SWCNTs and AmPy-12, which has been attributed to the disruption of π-conjugation by a conformational change,[34] does not change the nanotubes' electronic structure, thus implying that the electrical property of the SWCNTs remains basically unchanged after the functionalization with AmPy-12.

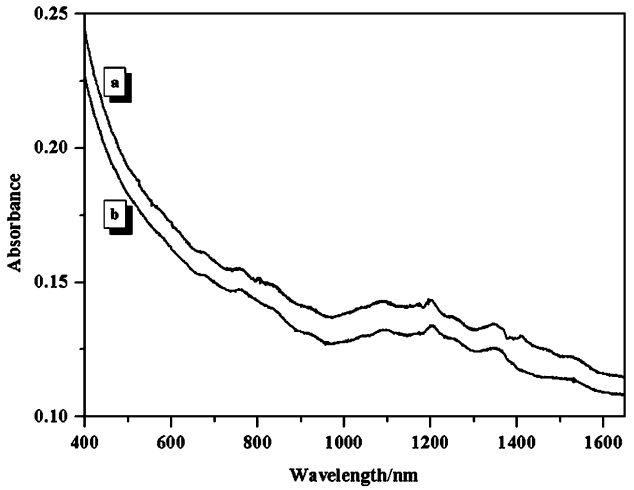

Fig. 7 UV-Vis-NIR spectra of the dispersions of (a) the SWCNTs and (b) SWCNT/AmPy-12 hybrid in THF.

The optimized SWCNT dispersion, which contains 75.4 mg L^{-1} of SWCNTs and 0.08 mg ml^{-1} of AmPy-12,[36] was used for the preparation of the epoxy composites. For comparison, the dispersion with an absence of AmPy-12 was also employed. Table 2 summarizes the mechanical properties of neat epoxy resin and its composites. Each datum reported here is an average of at least five measurements. With increasing SWCNT content, both the tensile strength and Young's modulus of the composites filled with AmPy-12-functionalized SWCNTs (SWCNT/EP–AmPy-12) increase and reach the maxima at a content of 0.3 wt %. Further increase of the SWCNT content leads to a weakening of tensile properties. The maximal tensile strength and Young's modulus were 51.55 ± 3.61 MPa and 2.01 ± 0.18 GPa, respectively, representing 54% and 27% increments relative to those of neat resin. In contrast, the SWCNT/EP composite acquires its optimal tensile strength (40.76 ± 4.71 MPa) and Young's modulus (1.77 ± 0.15 GPa) at 0.5 wt% nanotube content, which are 22% and 12% above neat resin and fall within a reasonable range considering the smooth and inert surface, as well as the intrinsically bundled nature of pristine SWCNTs. Moreover, it is observed that the addition of SWCNTs slightly increases the elongation at break, indicating that the toughness of EP is not weakened.

For exploring the reinforcement mechanism, the SEM study was performed on the fracture surface of SWCNT/EP–AmPy-12 composite with 0.3 wt% SWCNT content. As observed in Fig. 8a, the AmPy-12-functionalized SWCNTs are uniformly dispersed and tightly embedded in the epoxy matrix. A magnified observation shows that some nanotubes span the microcracks (Fig. 8b), suggesting strong interfacial adhesion between the epoxy matrix and SWCNTs. The strong interfacial interaction is further argued by nanotubes sheathed with epoxy resin (Fig. 8c). In the control study, SWCNTs form into agglomerates in the SWCNT/EP composite containing the same SWCNT content, displaying a very poor dispersing state (Fig. 8d). In addition, due to weak interfacial interactions, many nanotubes were pulled out from the matrix and float over the fracture surface (Figs 8d and e). It is well-known that good dispersion decreases the stress concentration centers, affords more uniform stress distribution and increases the interfacial area for efficient stress transfer.[1] A good interfacial adhesion between the nanotubes and matrix further enhances these effects.[37] From the SEM observation, application of AmPy-12 realizes both a uniform dispersion of nanotubes and their strong adhesion to the epoxy matrix, thus ensuring superior mechanical properties of the resultant composites. Even so, it should be pointed out that there exists an upper limit for AmPy-12-functionalized SWCNTs to be well-dispersed in the matrix. Fig. 8f reveals that SWCNTs tend to agglomerate, while the content increases to 0.5 wt%. Such observation makes a good response to the mechanical test results.

In the presence of AmPy-12, enhanced interfacial adhesion is attributed to the strong π–π interactions between the SWCNT and AmPy-12, as well as the covalent bonding of AmPy-12 with the epoxy matrix (Fig. 1). The formation of new bonds was confirmed by FTIR analyses. For easily detecting the reaction,

Table 2 Mechanical and thermal properties of neat epoxy resin and its composites. Datum within parentheses is % increase relative to neat resin.

SWNT content/wt (%)		0	0.1	0.2	0.3	0.5	1.0
Tensile Strength/ MPa	SWCNT/EP	33.4 ± 2.9	34.9 ± 3.0 (4)	36.3 ± 3.1 (9)	39.8 ± 4.3 (19)	40.8 ± 4.7 (22)	37.5 ± 4.5 (12)
	SWCNT/EP–AmPy-12		35.4 ± 3.7 (6)	42.4 ± 2.7 (27)	51.6 ± 3.6 (54)	47.2 ± 4.2 (41)	46.1 ± 4.4 (38)
Young's Modulus/ GPa	SWCNT/EP	1.68 ± 0.15	1.68 ± 0.17 (6)	1.67 ± 0.14 (6)	1.73 ± 0.16 (9)	1.77 ± 0.15 (12)	1.72 ± 0.17 (9)
	SWCNT/EP–AmPy-12		1.74 ± 0.15 (10)	1.80 ± 0.17 (14)	2.01 ± 0.18 (27)	1.89 ± 0.17 (20)	1.82 ± 0.18 (15)
Elongation at Break/%	SWCNT/EP	2.6 ± 0.2	2.6 ± 0.3 (0)	2.7 ± 0.2 (4)	2.8 ± 0.3 (8)	2.8 ± 0.3 (8)	2.8 ± 0.4 (8)
	SWCNT/EP–AmPy-12		2.7 ± 0.3 (4)	2.8 ± 0.3 (8)	3.4 ± 0.3 (31)	3.1 ± 0.3 (20)	3.1 ± 0.3 (20)
T_g/°C	SWCNT/EP	70	70	68	56	57	–
	SWCNT/EP–AmPy-12		75	73	70	62	–

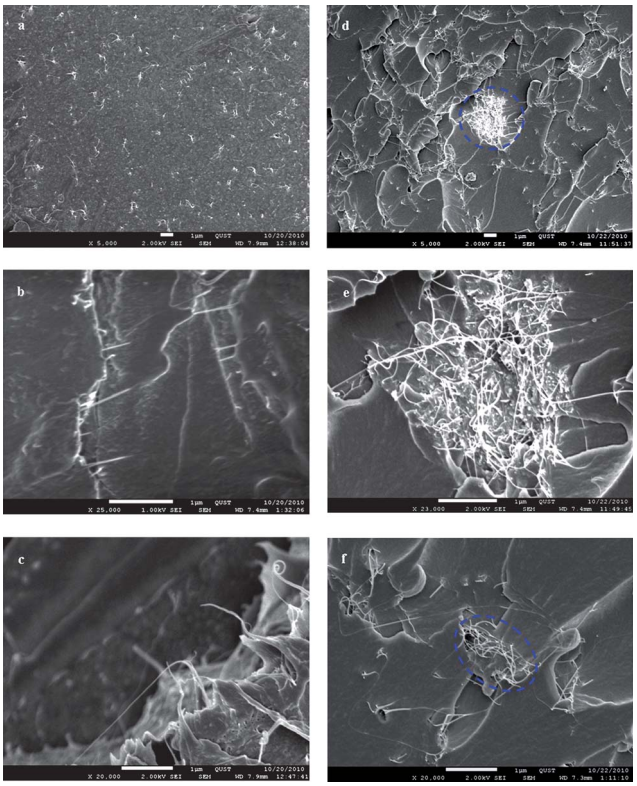

Fig. 8 SEM images of (a–c) SWCNT/EP–AmPy-12 composite with 0.3 wt% SWCNTs, (d) and (e) SWCNT/EP composite with 0.3 wt% SWCNTs and (f) SWCNT/EP–AmPy-12 composite with 0.5 wt% SWCNTs.

a blend containing a larger weight ratio of AmPy-12 to Epofix resin (60/40) was heated at the curing condition of composites. After heating, the viscous blend becomes a hard, but brittle solid. The FTIR spectra show that the bands for epoxy group (912 cm^{-1}) in Epofix resin (Fig. 9a) and for $–NH_2$ (3415 cm^{-1}) and –NH– (3290 cm^{-1}) species in AmPy-12 (Fig. 9b) still appear in the as-prepared blend (Fig. 9c), but cannot be detected anymore in the thermally treated sample (Fig. 9d). A new and broad peak centered at 3365 cm^{-1}, assigned to –OH stretching, presents in the spectrum of the treated sample (Fig. 9d), suggesting the reaction of AmPy-12 with Epofix resin.

The electrical conductivities of the composites were also characterized. As shown in Fig. 10a, the conductivities of both SWCNT/EP–AmPy-12 and SWCNT/EP significantly improve with increasing SWCNT content, showing a typical percolation behavior. The dependency of conductivities (σ) on SWCNT content (m) can be described using the scaling law[38]

$$\sigma = \sigma_0(m - m_c)^{\beta}, \text{ for } m > m_c \quad (1)$$

where m_c is the mass fraction at the percolation threshold, σ_0 and β are constants, and β should be close to 2 for a three dimensional (3D) percolating system.[39] To easily calculate the percolation threshold, eqn (1) is transformed to the logarithmic form of eqn (2):

$$\log\sigma = \beta\log(m - m_c) + \log\sigma_0 \quad (2)$$

By evaluating the linearity of the $\log\sigma$ *vs* $\log(m - m_c)$ graph until the lowest possible SWCNT content, the m_c values are determined to be 0.1 wt% ($\beta = 2.02$) for SWCNT/EP–AmPy-12 composites (Fig. 10b) and 0.4 wt% ($\beta = 1.99$) for SWCNT/EP composites (Fig. 10c). These values suggest that in the presence of AmPy-12, 0.1 wt% of SWCNTs in the epoxy matrix is already enough to form a 3D network as an effective conductive path. In the absence of AmPy-12, however, the dispersion quality of the SWCNTs becomes poor and more nanotubes (0.4 wt%) are required to construct the similar conductive path. One of the

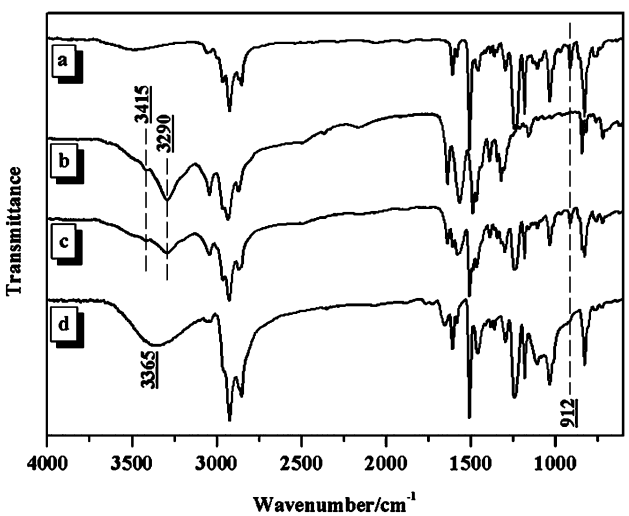

Fig. 9 FTIR spectra of (a) Epofix resin, (b) AmPy-12, (c) the as-prepared blend of AmPy-12 and Epofix resin (weight ratio of 60/40) and (d) thermally treated sample (blend in c) at 50 °C for 12 h and 80 °C for 2 h.

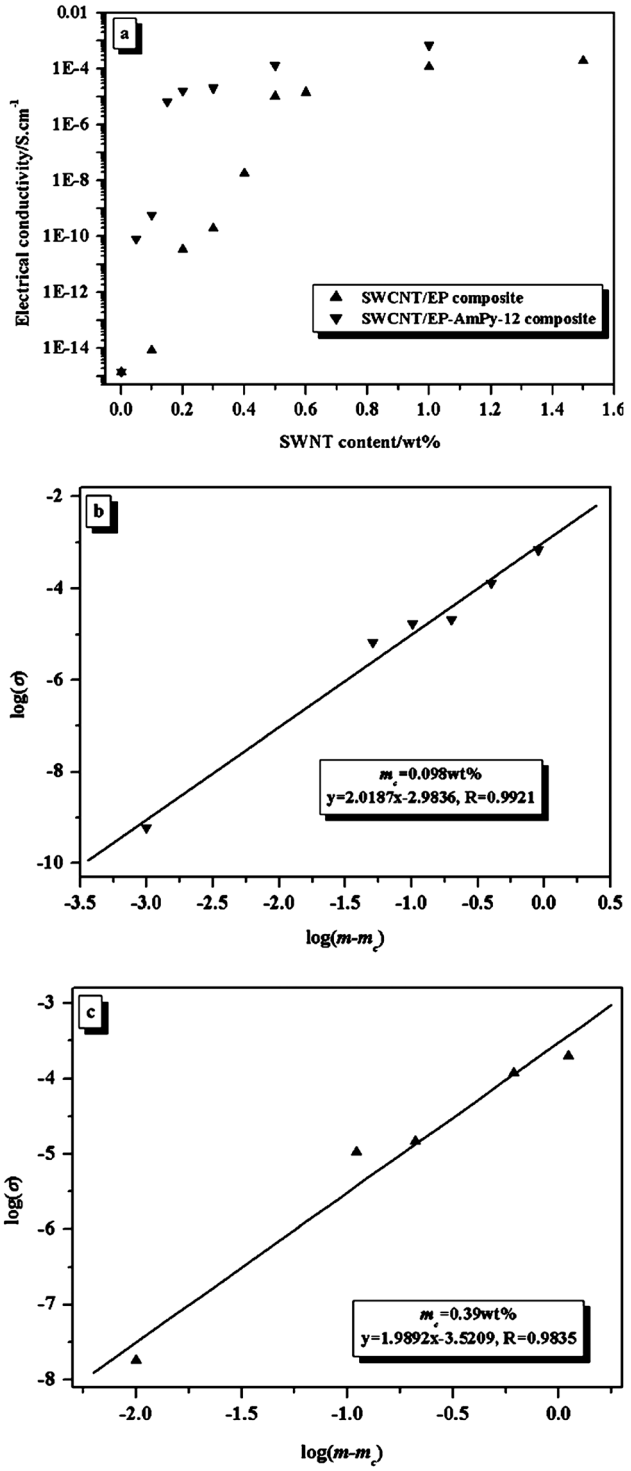

Fig. 10 (a) Electrical conductivity of the epoxy composites as a function of the SWCNT content (m) and the linear behavior of conductivity against ($m - m_c$) with m_c of (b) 0.098 wt% for the SWCNT/EP–AmPy-12 composite and (c) 0.39 wt% for the SWCNT/EP composite.

promising applications of the conductive composites is use as antistatic materials that demand a conductivity not lower than 10^{-8} S cm^{-1}.[40] For SWCNT/EP–AmPy-12, only 0.15 wt% of SWCNTs made the composite (with a conductivity of 6.7×10^{-6} S cm^{-1}) satisfy such an antistatic criterion. To attain the same criterion, however, about 8–20 wt% of carbon black should be added into epoxy resin.[41] This means that antistatic, but much lightweight epoxy composites are in prospect.

With addition of AmPy-12, the thermal properties (typically glass transition temperature (T_g) determined by DSC) of SWCNT/EP–AmPy-12 composites are improved relative to neat resin and SWCNT/EP composites (Table 2). The increased T_g results from the good nanotube dispersion and strong interfacial interaction, which restricts the segmental motion of epoxy-hardener molecules. Beyond 0.3 wt%, a further increase of the SWCNT content leads to the reduction of T_g, indicating the lower curing degree in the composite. This may possibly be due to the formation of SWCNT agglomerates (Fig. 8f) that in turn hinder the local curing reaction of epoxy with hardener.

4. Conclusions

Three reactive AmPys with various spacer chain lengths, *i.e.* AmPy-2, AmPy-6 and AmPy-12, were synthesized for engineering a SWCNT/epoxy matrix interface at a molecular level. The particularly designed amino group enables AmPy to be covalently bonded to the epoxy network, whereas the pyrene unit provides AmPy with the ability to be strongly adsorbed on the nanotube surface through π–π interactions. By setting two criterions of (1) the functionalization efficiency for pristine SWCNTs and (2) the dispersion stability, AmPy-12 was optimized for the preparation of epoxy composites. Due to homogeneous dispersion and enhanced interfacial interaction, only 0.3 wt% of SWCNTs increased the tensile strength and Young's modulus of the composite by 54% and 27%, respectively, over that of neat epoxy resin. A low electrical percolation threshold of 0.1 wt% SWCNTs and an improved thermal property were also observed. In comparison, the composite with an absence of AmPy-12 shows a 22% increment of the tensile strength and 12% of Young's modulus at an optimum SWCNT content of 0.5 wt%. The corresponding percolation threshold was up to 0.4 wt%. The application of AmPy-12 thus affords multifunctional, but lightweight epoxy composites. Finally, the concept of Interface Molecular Engineering of the CNT/epoxy composite system demonstrated here may be easily extended to other CNT/polymer systems, providing a general strategy for developing high-quality CNT/polymer composites.

Acknowledgements

The financial support from NSF of China (No. 20704024 and 51173091), NSF of Shandong province (No. Q2007F08) and Taishan Mountain Scholar Constructive Engineering Foundation are gratefully acknowledged. Y. H. Yan would also like to thank the Alexander-von-Humboldt-Stiftung (Germany) for a fellowship.

Notes and references

1 J. N. Coleman, U. Khan and Y. K. Gun'ko, *Adv. Mater.*, 2006, **18**, 689.
2 M. Moniruzzaman and K. I. Winey, *Macromolecules*, 2006, **39**, 5194.
3 N. G. Sahooa, S. Ranab, J. W. Chob, L. Li and S. H. Chana, *Prog. Polym. Sci.*, 2010, **35**, 837.
4 M. T. Byrne and Y. K. Gun'ko, *Adv. Mater.*, 2010, **22**, 1672.

5 D. Tasis, N. Tagmatarchis, A. Bianco and M. Prato, *Chem. Rev.*, 2006, **106**, 1105.
6 Y. Lin, M. J. Meziani and Y. P. Sun, *J. Mater. Chem.*, 2007, **17**, 1143.
7 J. T. Sun, C. Y. Hong and C. Y. Pan, *Polym. Chem.*, 2011, **2**, 998.
8 J. Chen, R. Ramasubramaniam, C. Xue and H. Liu, *Adv. Funct. Mater.*, 2006, **16**, 114.
9 A. A. Mamedov, N. A. Kotov, M. Prato, D. M. Guldi, J. P. Wicksted and A. Hirsch, *Nat. Mater.*, 2002, **1**, 190.
10 K. T. Kim and W. H. Jo, *J. Polym. Sci., Part A: Polym. Chem.*, 2010, **48**, 4184.
11 K. T. Kim and W. H. Jo, *Carbon*, 2009, **47**, 1126.
12 D. M. Delozier, K. A. Watson Jr, J. G. Smith, T. C. Clancy and J. W. Connell, *Macromolecules*, 2006, **39**, 1731.
13 W. Yuan, J. Feng, Z. Judeh, J. Dai and M. B. Chan-Park, *Chem. Mater.*, 2010, **22**, 6542.
14 X. Y. Gong, J. Liu, S. Baskaran, R. D. Voise and J. S. Young, *Chem. Mater.*, 2000, **12**, 1049.
15 S. Cui, R. Canet, A. Derre, M. Couzi and P. Delhaes, *Carbon*, 2003, **41**, 797.
16 R. A. Graff, J. P. Swanson, P. W. Barone, S. Baik, D. A. Heller and M. S. Strano, *Adv. Mater.*, 2005, **17**, 980.
17 S. Wang, Z. Liang, P. Gonnet, Y. H. Liao, B. Wang and C. Zhang, *Adv. Funct. Mater.*, 2007, **17**, 87.
18 L. Liu, K. C. Etika, K. S. Liao, L. A. Hess, D. E. Bergbreiter and J. C. Grunlan, *Macromol. Rapid Commun.*, 2009, **30**, 627.
19 T. Morishita, M. Matsushita, Y. Katagiri and K. Fukumori, *Carbon*, 2009, **47**, 2716.
20 D. K. Choi, S. H. Jin and D. S. Lee, *Macromol. Symp.*, 2008, **264**, 100.
21 K. C. Etika, F. D. Jochum, M. A. Cox, P. Schattling, P. Theato and J. C. Grunlan, *Macromolecules*, 2010, **43**, 9447.
22 T. J. Simmons, J. Bult, D. P. Hashim, R. J. Linhardt and P. M. Ajayan, *ACS Nano*, 2009, **3**, 865.
23 Y. H. Yan, J. Cui, P. Poetschke and B. Voit, *Carbon*, 2010, **48**, 2603.
24 J. L. Bahr, E. T. Mickelson, M. J. Bronikowski, R. E. Smalley and J. M. Tour, *Chem. Commun.*, 2001, 193.
25 Y. H. Yan, S. B. Yang, J. Cui, L. Jakisch, P. Poetschke and B. Voit, *Polym. Int.*, 2011, **60**, 1425.
26 B. Vigolo, A. Penicaud, C. Coulon, C. Sauder, R. Pailler, C. Journet, P. Bernier and P. Poulin, *Science*, 2000, **290**, 1331.
27 The fluorescence measurements provide some indirect evidence for the formation of supramolecular structures. In a typical measurement, for example, the weak and broad excimer emission (max. 475 nm) appears in the spectrum of the dispersion containing 0.15 mg ml^{-1} of AmPy-12 and 62.2 mg L^{-1} of SWCNTs, whereas only the monomer emission is visible for the dispersion containing 0.08 mg ml^{-1} of AmPy-12 and 75.4 mg L^{-1} of SWCNTs (Fig. S2†). Such observations imply that it is highly possible to form some supramolecular structures, such as dimers and multimers, in the dispersion if only the concentration of AmPy is high enough.
28 J. M. Bonard, T. Stora, J. P. Salvetat, F. Maier, T. Stöckli, C. Duschl, L. Forró, W. A. de Heer and A. Châtelain, *Adv. Mater.*, 1997, **9**, 827.
29 D. C. Dong and M. A. Winnik, *Photochem. Photobiol.*, 1982, **35**, 17.
30 D. C. Dong and M. A. Winnik, *Can. J. Chem.*, 1984, **62**, 2560.
31 M. Assali, M. Leal, I. Fernández, R. Baati, C. Mioskowski and N. Khiar, *Soft Matter*, 2009, **5**, 948.
32 T. Ogoshi, Y. Takashima, H. Yamaguchi and A. Harada, *J. Am. Chem. Soc.*, 2007, **129**, 4878.
33 D. Wang, W. X. Ji, Z. C. Li and L. Chen, *J. Am. Chem. Soc.*, 2006, **128**, 6556.
34 Q. Yang, S. Li, J. Zhou, F. Lu and X. Pan, *J. Phys. Chem. B*, 2008, **112**, 12934.
35 M. J. O'Connell, S. M. Bachilo, C. Huffman, V. C. Moore, M. S. Strano, E. H. Haroz, K. L. Rialon, P. J. Boul, W. H. Noon, C. Kittrell, J. Ma, R. H. Hauge, R. B. Weisman and R. E. Smalley, *Science*, 2002, **297**, 593.
36 The amount of AmPy-12 introduced in the preparation of the SWCNT/EP–AmPy-12 composites is equivalent to increasing the weight ratio of Epofix resin/hardener from 25 : 3 to 25 : 3.005–3.05 (3.005 for the composite containing 0.1 wt% SWCNTs and 3.05 for 1.0 wt% SWCNTs). This means that the deviations in the stoichiometry are in the order of less than 1% for most samples, except the one containing 1.0 wt% SWCNTs. Therefore, its effect on the later mechanical and thermal characterization is neglected.
37 M. Moniruzzaman, J. Chattopadhyay, W. E. Billups and K. I. Winey, *Nano Lett.*, 2007, **7**, 1178.
38 A. Clauset, C. R. Shalizi and M. E. J. Newman, *SIAM Rev.*, 2009, **51**, 661.
39 S. Barrau, P. Demont, A. Peigney, C. Laurent and C. Lacabanne, *Macromolecules*, 2003, **36**, 5187.
40 S. Stankovich, D. A. Dikin, G. H. B. Dommett, K. M. Kohlhass, E. J. Zimney, E. A. Stach, R. D. Piner, S. T. Nguyen and R. S. Ruoff, *Nature*, 2006, **442**, 282.
41 B. Pötshke, T. D. Fornes and D. R. Paul, *Polymer*, 2002, **43**, 3247.

